A novel research on the base force element method of complementary energy principle for finite strain problems

*Zhonghai Li, and †Yijiang Peng

Key Laboratory of Urban Security and Disaster Engineering Ministry of Education, Beijing University of Technology, Beijing, P. R. China

*Presenting author: lizhonghai@emails.bjut.edu.cn †Corresponding author: pengyijiang@bjut.edu.cn

Abstract

The finite element method based on the complementary energy principle and its combination with artificial neural networks is a worthwhile research topic. A new Base Force Element Method (BFEM) model is proposed in this study, which can solve the problems of large elastic deformation and finite strain in incompressible hyperelastic materials. The complementary energy function of nonlinear elasticity has not yet been proposed. The complementary energy function is replaced by a pre-trained Back-Propagation (BP) neural network to establish the constitutive relationship. This makes it easy for finite strain problems to be studied by the BFEM model. When the constitutive relationships of different incompressible hyperelastic materials were described, only two parameters needed to be changed. The governing equations of the BFEM model are general and concise, and its derivation process does not involve an approximate representation of shape functions. The calculation results of the examples indicate that the model has high accuracy. This new numerical method fills the gap in using the complementary energy finite element method to calculate the finite strain problem of incompressible hyperelastic materials.

Keywords: Complementary energy principle, BFEM, large elastic deformation, finite strain, BP neural network, solid element

Introduction

When the nonlinear complementary energy variational principle is established by the second type of Piola-Kirchhoff stress tensor, a coupling term containing force and displacement appears in its integral term [1]. This makes it difficult for numerical methods based on the complementary energy principle to solve geometric nonlinear problems. This difficulty is overcome by the base force [2]. Traditional stress tensors can be replaced by base force to describe the stress state at a certain point [3]. The coupling term is eliminated in the process of establishing the complementary energy principle using base force. According to the complementary energy principle of base force, a new finite element method - BFEM is proposed [2]. This is a new way of calculating nonlinear solid mechanics. Recently, BFEM has been used to accurately solve the large elastic deformation problems of trusses and analyze the stability of beams [4, 5]. The constitutive relationship used in BFEM is still linear and elastic, the research problems are still limited to the range of linear elastic materials.

Many scholars have proposed strain energy functions to characterize the constitutive relationships of nonlinear elasticity [6-8]. However, the complementary energy function of nonlinear elasticity has not yet been proposed. This makes it difficult to solve finite strain problems using complementary energy finite element methods. The strain energy functions are established based on the phenomenological method [9-11]. These functions are mostly represented by strain invariants or principal tensile ratios. Similarly, can the complementary

energy function be represented by stress invariants or principal stress? The answer is yes when the constitutive relationship is linear elastic. The linear complementary energy function is obtained using the Legendre transformation. If the constitutive relationship is nonlinear elastic, it is difficult to obtain the corresponding complementary energy function using the Legendre transformation. This is because the constitutive relationship must be inverted during the derivation of the complementary energy function, but the nonlinear constitutive relationship may not be reversible [12, 13]. To avoid this difficulty, complementary energy functions can be established through phenomenological methods. However, if the material is replaced, it is necessary to fit and analyze the sample again, so the generality of this method is poor. Neural networks have excellent data feature extraction capabilities [14-16], reducing the cost of manual processing of samples. When the material is replaced, the neural network only needs to be retrained based on different samples. Therefore, using constitutive relationships formed by neural networks to establish the complementary energy principle of finite strain is a general method.

To solve the finite strain problems of incompressible hyperelastic materials using complementary finite element models, a BFEM based on constitutive relationships established by BP neural networks is proposed. The premise of the complementary energy function obtained by Legendre transformation is that the nonlinear constitutive relationship is reversible. By using the BP neural network, the strain-stress relationship can be directly obtained, avoiding the use of the Legendre transform. To provide training data to the BP neural network, the test samples were inverted. The weights and biases are extracted from the pre-trained BP neural network and substituted into the mathematical expression of the BP neural network. The two unknown parameters in the element compliance matrix can be predicted by this expression. In this way, the governing equations are complete and the finite strain problems of incompressible materials can be solved.

BFEM model

Assuming that σ and τ are the Cauchy stress tensor and Piola stress tensor, respectively. These stress tensors can be represented by the base force T^i as follows [2]:

$$\boldsymbol{\sigma} = \frac{1}{V_O} \boldsymbol{T}^i \otimes \boldsymbol{Q}_i \,, \tag{1}$$

$$\boldsymbol{\tau} = \frac{1}{V_p} \boldsymbol{T}^i \otimes \boldsymbol{P}_i, \qquad (2)$$

where P_i and Q_i are the covariant vector bases of the initial configuration and the deformed configuration, respectively, V_P and V_Q are the base volumes before and after deformation. Assuming that the volume of an elastic body is represented by V, its boundary S can be divided into Dirichlet boundary S_u and Neumann boundary S_σ . Both boundaries satisfy the conditions $S_u \cup S_\sigma = S$ and $S_u \cap S_\sigma = \varnothing$. m is the unit normal vector on boundary S_u and \overline{u} is the given displacement. The complementary energy principle of base force [17] is

$$\int_{V} W_{c}\left(\boldsymbol{T}^{i}\right) dV - \int_{S_{u}} \frac{\boldsymbol{m}_{i}}{V_{p}} \boldsymbol{\overline{u}} \cdot \boldsymbol{T}^{i} dS , \qquad (3)$$

where $m_i = \mathbf{P}_i \cdot \mathbf{m}$, and W_c is the complementary energy function. Since \mathbf{T}^i and displacement gradients \mathbf{u}_i are conjugated,

$$\frac{1}{V_P} \boldsymbol{T}^i \cdot \boldsymbol{u}_i = W_c + W \,, \tag{4}$$

where W is the strain energy function. Similar to the polar decomposition of deformation gradients, u_i can be divided into [18]

$$\boldsymbol{u}_{i} = \boldsymbol{u}_{id} + \boldsymbol{u}_{ir}, \qquad (5)$$

where u_{id} is the deformation displacement gradients, and u_{ir} is the rotation displacement gradients. Therefore, formula (4) is divided into

$$W_{cd} = \frac{1}{V_P} \mathbf{T}^i \cdot \mathbf{u}_{id} - W, \quad W_{cr} = \frac{1}{V_P} \mathbf{T}^i \cdot \mathbf{u}_{ir} , \qquad (6)$$

where W_{cd} is the deformed part of W_c , and W_{cr} is the rotating part of W_c . The complementary energy principle of large elastic deformation represented by T^i is obtained by substituting formula (6) into formula (3). It is worth noting that W_{cd} should be a specific expression rather than the form presented by formula (6)₁. For example, the W_{cd} of linear elastic materials can be expressed by the first invariant J_1 and the second invariant J_2 of the stress tensor σ :

$$W_{cd}\left(\mathbf{T}^{i},\theta\right) = \frac{1+\nu}{2E} \left(J_{2} - \frac{\nu}{1+\nu}J_{1}^{2}\right),\tag{7}$$

where θ is the rotation angle, v is the Poisson's ratio, and E is the Young's modulus. Let us assume that the W_{cd} of incompressible hyperelastic materials is

$$W_{cd} = W_{cd} \left(J_{1\tau}, J_{2\tau} \right), \tag{8}$$

where $J_{1\tau}$ and $J_{2\tau}$ are the first and second invariants of stress τ , respectively. The complementary energy of the element is

$$W_{cd}^{e} = \int_{V} W_{cd} \left(J_{1\tau}, J_{2\tau} \right) dV .$$
 (9)

The average Piola stress of the element is

$$\overline{\tau} = \frac{1}{V} \int_{V} \tau dV = \frac{1}{V} \int_{V} \frac{1}{V_{p}} T^{i} \otimes N_{i} dV , \qquad (10)$$

where N_i is the covariant vector base of the intermediate configuration after rotation, $N_i = P_i + u_{ir}$. According to the Gaussian theorem, formula (10) is rewritten as

$$\overline{\tau} = \frac{1}{V} \int_{A} T \otimes N dS , \qquad (11)$$

where T is the stress vector acting on boundary A, and N is the intermediate position vector of the T action point. If the element is small enough, it can be approximately assumed that the stress is evenly distributed on each surface. The area integral in formula (11) can be eliminated:

$$\overline{\tau} = \frac{1}{V} T^{\alpha} \otimes N_{\alpha}, \tag{12}$$

where α is the label of the surface of the element, and $N_{\alpha} = \mathbf{R} \cdot \mathbf{P}_{\alpha}$ is the intermediate position vector of the midpoint in surface α . Formula (12) satisfies the Einstein summation convention. According to formulas (10) and (12),

$$\int_{V} J_{1\tau} dV = \int_{V} \tau dV : \mathbf{I} = V \overline{\tau} : \mathbf{I} = \mathbf{T}^{\alpha} \cdot \mathbf{N}_{\alpha} , \qquad (13)$$

$$\int_{V} J_{2\tau} dV = \int_{V} \tau dV : \int_{V} \tau dV = V^{2} \overline{\tau} : \overline{\tau} = (T^{\alpha} \cdot T^{\beta}) (N_{\alpha} \cdot N_{\beta}).$$
(14)

Let us assume that the first and second invariants of stress $\bar{\tau}$ are

$$J_{1T} = \overline{\tau} : I = \frac{1}{V} T^{\alpha} \cdot N_{\alpha}$$
 (15)

and

$$J_{2T} = \overline{\tau} : \overline{\tau} = \frac{1}{V^2} (T^{\alpha} \cdot T^{\beta}) (N_{\alpha} \cdot N_{\beta}), \qquad (16)$$

respectively. Therefore, the complementary energy form of elements is approximately

$$\int_{V} W_{cd} \left(J_{1\tau}, J_{2\tau} \right) dV \approx W_{cd}^{e} \left(J_{1T}, J_{2T} \right). \tag{17}$$

Similarly,

$$W_{cr}^{e} = \int_{V} W_{cr} dV = \boldsymbol{T}^{\alpha} \cdot \boldsymbol{u}_{\alpha r} = \boldsymbol{T}^{\alpha} \cdot (\boldsymbol{R} - \boldsymbol{I}) \cdot \boldsymbol{P}_{\alpha}, \qquad (18)$$

where $u_{\alpha r}$ is the rotating part of the displacement of the midpoint in surface α , and R is the rotation tensor. According to the Gaussian theorem, formulas (3), (4), (6), (17), and (18), the complementary function of an element is

$$\boldsymbol{\pi}_{C} = W_{cd}^{e} \left(\boldsymbol{J}_{1T}, \boldsymbol{J}_{2T} \right) + W_{cr}^{e} - \overline{\boldsymbol{u}}_{\alpha} \cdot \boldsymbol{T}^{\alpha} , \qquad (19)$$

where $\overline{\boldsymbol{u}}_{\alpha}$ is the given displacement of the midpoint in surface α . The element surface force \boldsymbol{T}^{α} needs to meet the following constraint conditions:

$$\sum_{\alpha} T^{\alpha} = 0 \qquad \text{(Without body force)}$$

$$T^{S_{\sigma}} = \overline{T} \qquad \text{(On } S_{\sigma}) \qquad , \qquad (20)$$

$$T^{S_{\alpha}} = T^{S_{\beta}} \qquad \text{(On } S_{\alpha\beta})$$

where $S_{\alpha\beta}$ is the adjacent edge between elements. The Lagrange multiplier method is used to relax the constraints (20)₁. The modified complementary functional of elements is obtained:

$$\boldsymbol{\pi}_{c}^{*}\left(\boldsymbol{T},\boldsymbol{\theta},\boldsymbol{L}\right) = W_{cd}^{e}\left(\boldsymbol{J}_{1T},\boldsymbol{J}_{2T}\right) + W_{cr}^{e} + \boldsymbol{L}\left(\sum_{\alpha}\boldsymbol{T}^{\alpha}\right) - \boldsymbol{\bar{u}}_{\alpha} \cdot \boldsymbol{T}^{\alpha}, \tag{21}$$

where L are Lagrange multipliers. The constraints $(20)_2$ and $(20)_3$ can be satisfied in programming. If an elastic body is composed of n elements, the modified complementary energy function is

$$\Pi_c^* = \sum_{n} \left[\pi_c^* \left(\boldsymbol{T}, \boldsymbol{\theta}, \boldsymbol{L} \right) \right]. \tag{22}$$

The stationary value is taken for formula (21) before assembly. The finite element governing equations are

$$\begin{cases}
\frac{\partial \pi_c^*}{\partial \boldsymbol{T}^{\alpha}} = \boldsymbol{C}_{\alpha\beta} \cdot \boldsymbol{T}^{\beta} + (\boldsymbol{R} - \boldsymbol{I}) \cdot \boldsymbol{P}_{\alpha} + \boldsymbol{L} - \overline{\boldsymbol{u}}_{\alpha} \\
\frac{\partial \pi_c^*}{\partial \theta} = \frac{\partial W_{cd}^e}{\partial \theta} + \boldsymbol{T}^{\alpha} \cdot \frac{d\boldsymbol{R}}{d\theta} \cdot \boldsymbol{P}_{\alpha} \\
\frac{\partial \pi_c^*}{\partial \boldsymbol{L}} = \sum_{\alpha} \boldsymbol{T}^{\alpha}
\end{cases} , \tag{23}$$

where $C_{\alpha\beta}$ is the compliance matrix. The complementary energy function, $C_{\alpha\beta}$, and $\partial W_{cd}^e/\partial\theta$ of linear elastic materials are specific. Although the complementary energy function of hyperelastic materials is unknown, $C_{\alpha\beta}$ and $\partial W_{cd}^e/\partial\theta$ with unknown parameters can still be derived according to the formula (17). According to the chain rule,

$$\frac{\partial W_{cd}^{e}\left(\boldsymbol{J}_{1T},\boldsymbol{J}_{2T}\right)}{\partial \boldsymbol{T}^{\alpha}} = \frac{\partial W_{cd}^{e}}{\partial \left(\boldsymbol{J}_{1T}\right)^{2}} \frac{\partial \left(\boldsymbol{J}_{1T}\right)^{2}}{\partial \boldsymbol{T}^{\alpha}} + \frac{\partial W_{cd}^{e}}{\partial \boldsymbol{J}_{2T}} \frac{\partial \boldsymbol{J}_{2T}}{\partial \boldsymbol{T}^{\alpha}} = \frac{2w_{\mu}}{V^{2}} \left(\boldsymbol{N}_{\alpha} \otimes \boldsymbol{N}_{\beta}\right) \cdot \boldsymbol{T}^{\beta} + \frac{2w_{\mu}}{V^{2}} p_{\alpha\beta} \boldsymbol{T}^{\beta}, \quad (24)$$

where

$$W_{1t} = \partial W_{cd}^e / \partial \left(J_{1T} \right)^2, \tag{25}$$

$$W_{2t} = \partial W_{cd}^e / \partial J_{2T} . {26}$$

Similarly,

$$\frac{\partial W_{cd}^{e}\left(J_{1T},J_{2T}\right)}{\partial \theta} = \frac{\partial W_{cd}^{e}}{\partial \left(J_{1T}\right)^{2}} \frac{\partial \left(J_{1T}\right)^{2}}{\partial \theta} = \frac{2w_{lt}}{V^{2}} \left(\boldsymbol{T}^{\alpha} \cdot \boldsymbol{N}_{\alpha}\right) \left(\boldsymbol{T}^{\beta} \cdot \frac{d\boldsymbol{N}_{\beta}}{d\theta}\right). \tag{27}$$

In formula (16),

$$N_{\alpha} \cdot N_{\beta} = P_{\alpha} \cdot P_{\beta} \,, \tag{28}$$

which makes $\partial J_{2T} / \partial \theta = 0$ in formula (27). The parameters w_{1t} and w_{2t} are functions with J_{1T} and J_{2T} as basic unknowns. According to formula (24), it is not difficult to see that the element compliance matrix derived from formula (17) is

$$C_{\alpha\beta} = \frac{2}{V^2} \left[w_{1t} \left(N_{\alpha} \otimes N_{\beta} \right) + w_{2t} p_{\alpha\beta} I \right]. \tag{29}$$

Because the complementary energy function W_{cd}^e can take any form with J_{1T} and J_{2T} as independent variables, formula (29) is a general expression for the element compliance matrix. When selecting different materials, w_{1t} and w_{2t} only need to be changed. If

$$w_{1t} = -\frac{vV}{2E}, w_{2t} = \frac{(1+v)V}{2E},$$
 (30)

 $C_{\alpha\beta}$ and $\partial W_{cd}^e/\partial\theta$ are suitable for linear elastic materials.

BP neural network embedded in BFEM model

According to the derivation in Section 2, the parameters w_{1t} and w_{2t} are crucial for describing the constitutive relationship. They are functions with J_{1T} and J_{2T} as basic unknowns:

$$W_{1t} = W_{1t} (J_{1T}, J_{2T}), \quad W_{2t} = W_{2t} (J_{1T}, J_{2T}).$$
 (31)

This mapping is described by a BP neural network, with J_{1T} and J_{2T} as inputs and w_{1t} and w_{2t} as outputs. The expression for a BP neural network with n layers is

$$\mathbf{x}_{1} = \begin{bmatrix} J_{1T}, J_{2T} \end{bmatrix}^{\mathrm{T}}$$

$$\mathbf{x}_{2} = f_{2} \left(\mathbf{H}^{(2,1)} \cdot \mathbf{x}_{1} + \mathbf{b}^{(2,1)} \right)$$

$$\mathbf{M}$$

$$\mathbf{x}_{n} = f_{n} \left(\mathbf{H}^{(n,n-1)} \cdot \mathbf{x}_{n-1} + \mathbf{b}^{(n,n-1)} \right) = \begin{bmatrix} w_{1t}, w_{2t} \end{bmatrix}^{\mathrm{T}}$$
(32)

where $\mathbf{H}^{(i,i-1)}$ is the weight matrix, $\mathbf{b}^{(i,i-1)}$ is the deviation vector, and f_i is the activation function. Their superscripts i and i-1 represent the layer number, i = 2,3... n. The activation function for each layer is

$$f_{i}(y) = \begin{cases} \frac{2}{1 + e^{-2y}} - 1 & i < n \\ y & i = n \end{cases}$$
 (33)

They enable the neural network to have nonlinear mapping ability. During the training process of neural networks, the weight matrix and deviation vector of each layer are updated using the gradient descent method until the error function is less than an acceptable error. If there are m sets of reference data, the error function is

$$\operatorname{Err}(\boldsymbol{H}, \boldsymbol{b}) = \frac{1}{2m} \sum_{k=1}^{m} \left[\left(\hat{w}_{1t}^{k} - w_{1t}^{k} \right)^{2} + \left(\hat{w}_{2t}^{k} - w_{2t}^{k} \right)^{2} \right], \tag{34}$$

where \hat{w}_{1t}^k and \hat{w}_{2t}^k are the predicted values of the neural network, and w_{1t}^k and w_{2t}^k are the reference values. The training process of the BP neural network and the calculation process of the BFEM model are shown in Fig. 1, and c is a set of weight matrices and deviation vectors for each layer. When iteratively updating the basic unknowns, it is necessary to recalculate J_{1T} and J_{2T} for each element to obtain the predicted values of w_{1t} and w_{2t} . The predicted values are substituted into equation (23) to test whether the new basic unknowns satisfy the control equations.

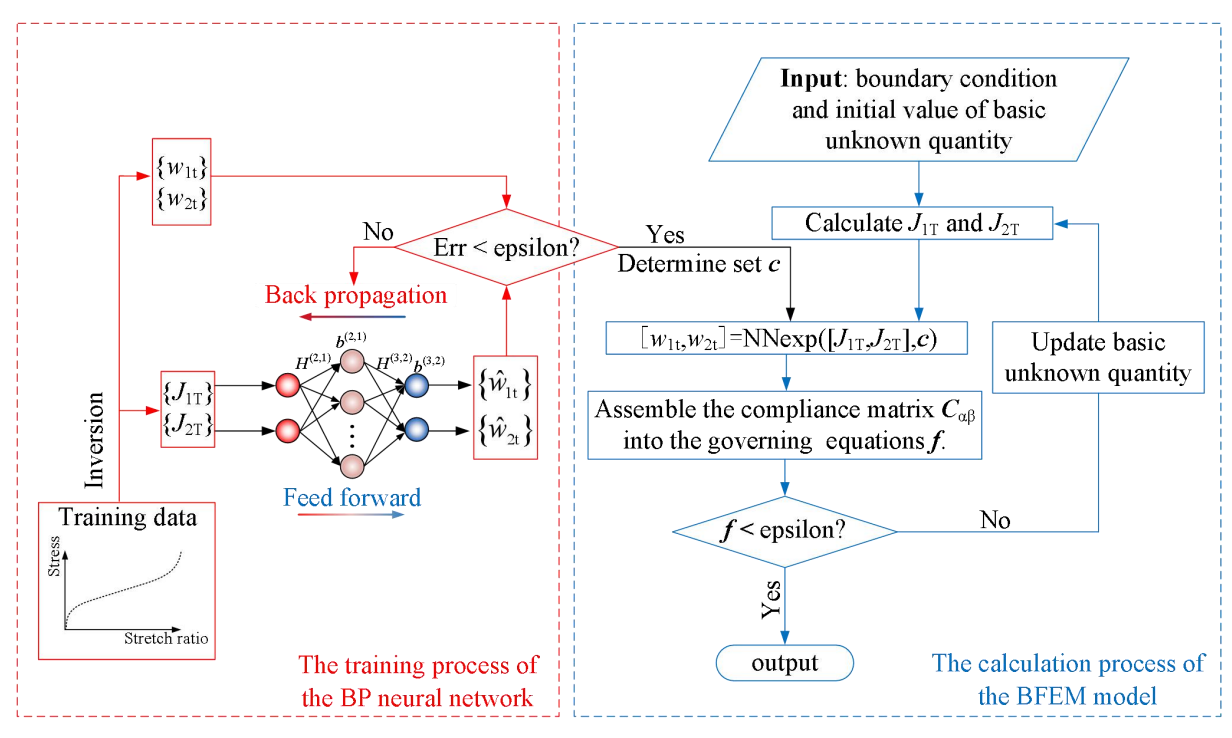


Figure 1. Training of BP Neural Network and BFEM solution flowchart

Example: stretching of a plate with a defect in the center

The top of the hyperelastic material plate with a defect in the center is subjected to a uniformly distributed load P. Due to the symmetry of structure and force, half of the plate is used for numerical research. The size, constraints, and mesh generation of the structure are shown in Fig. 2. To provide data and make comparisons, the constitutive relationship of this structure was established using the Mooney-Rivlin model [19]. This model is represented as

$$W = C_1(I_1 - 3) + C_2(I_2 - 3), (35)$$

where the parameter C_1 is 0.805 MPa and C_2 is 0.194 MPa. The training samples of the neural network were obtained by further inverting the uniaxial stretching data (stretching ratio of 1-6). A pre-trained BP neural network with 2 hidden layers and 7 neurons per layer is used to establish a new constitutive relationship. The mean squared errors of the training set, validation set, and test set are recorded in Fig. 3. It can be seen that the mean squared errors of the three sets are close to 10^{-15} , indicating good training results. Compare the vertical displacement of points A and B (marked in Fig. 2) with the results of the CPS8R element in Abaqus and record them in Fig. 4. The relative error of point A is 4.32%, and the relative error of point B is 3.62% when P = 2 MPa.

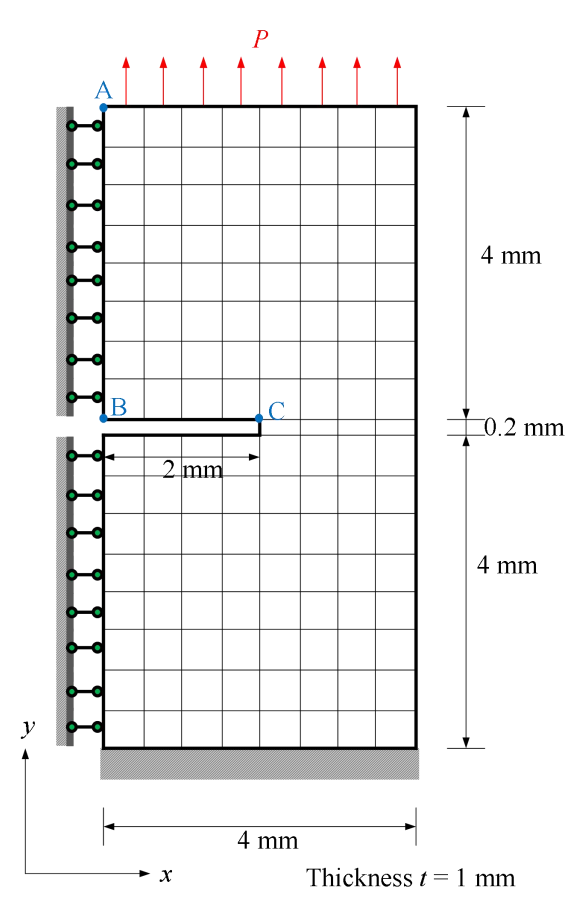


Figure 2. Plate with center defect (1/2 part)

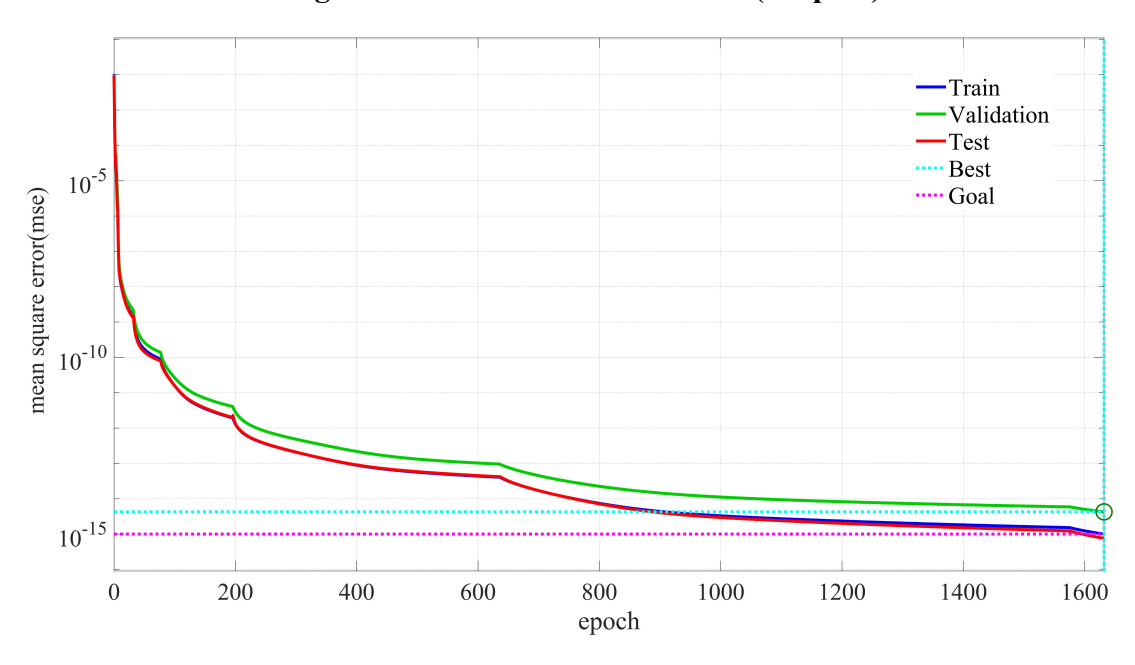


Figure 3. Mean squared error during the BP neural network training process

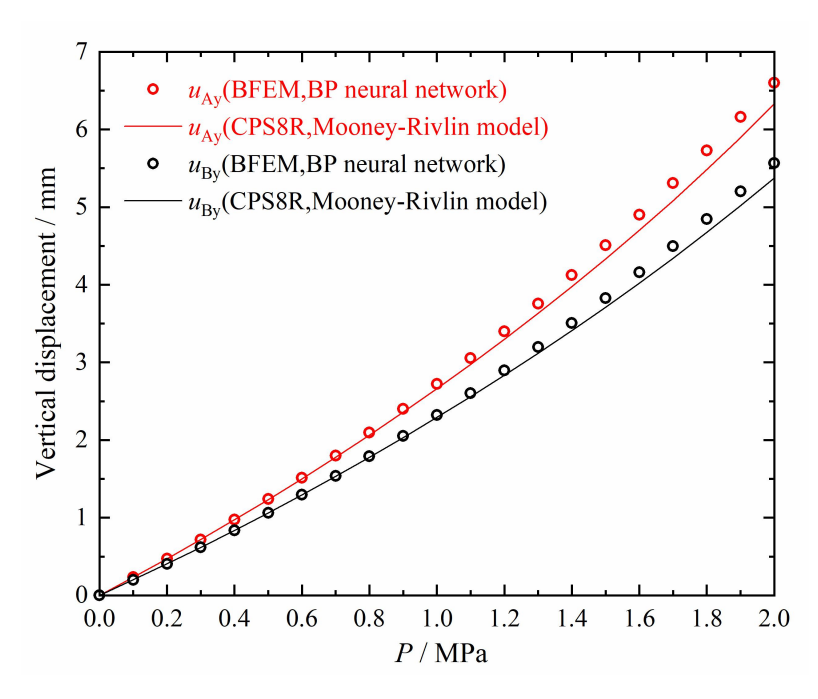


Figure 4. The vertical displacement of points A and B and the results of CPS8R element

As P increases, the stress of each element and the deformation contour are recorded in Fig. 5-7. From these figures, it can be seen that there is a clear phenomenon of stress concentration at the defect. In Fig. 5, there are higher stresses along the positive x-axis at the bottom of the structure and near point C, and higher stresses along the negative x-axis near point C. In Fig. 6, the stress σ_{yy} in the area from point C to point C gradually becomes smaller. In Fig. 7, the direction of stress σ_{xy} is opposite at the upper and lower edges of the defect. The obvious tensile deformation occurs on the overall structure, and the obvious rotation occurs on the elements around the defect (such as the C edge).

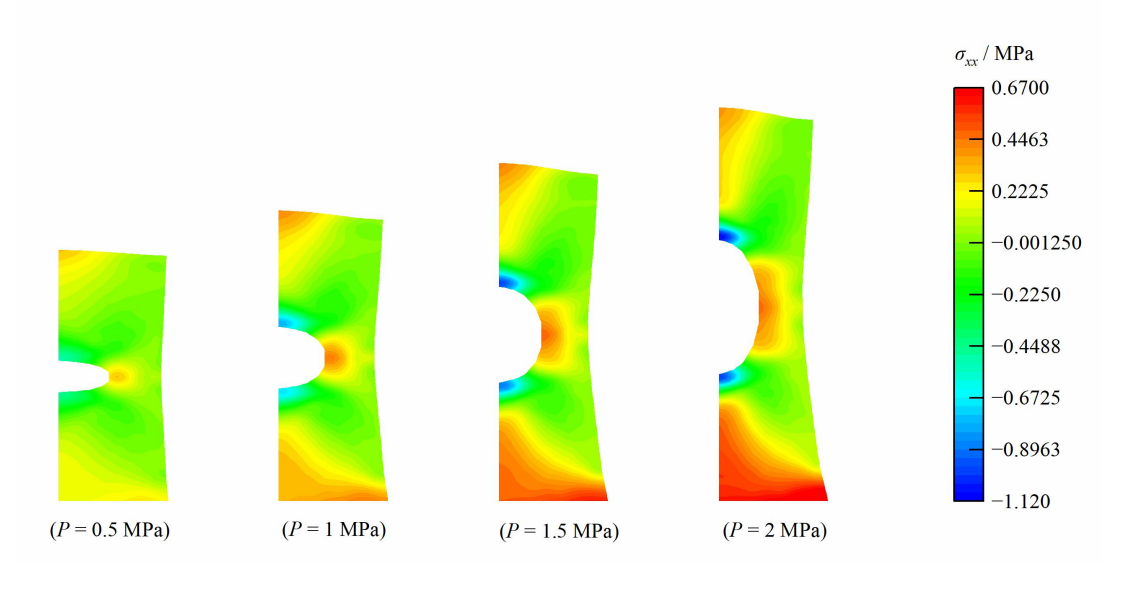


Figure 5. Stress σ_{xx} and deformation contour

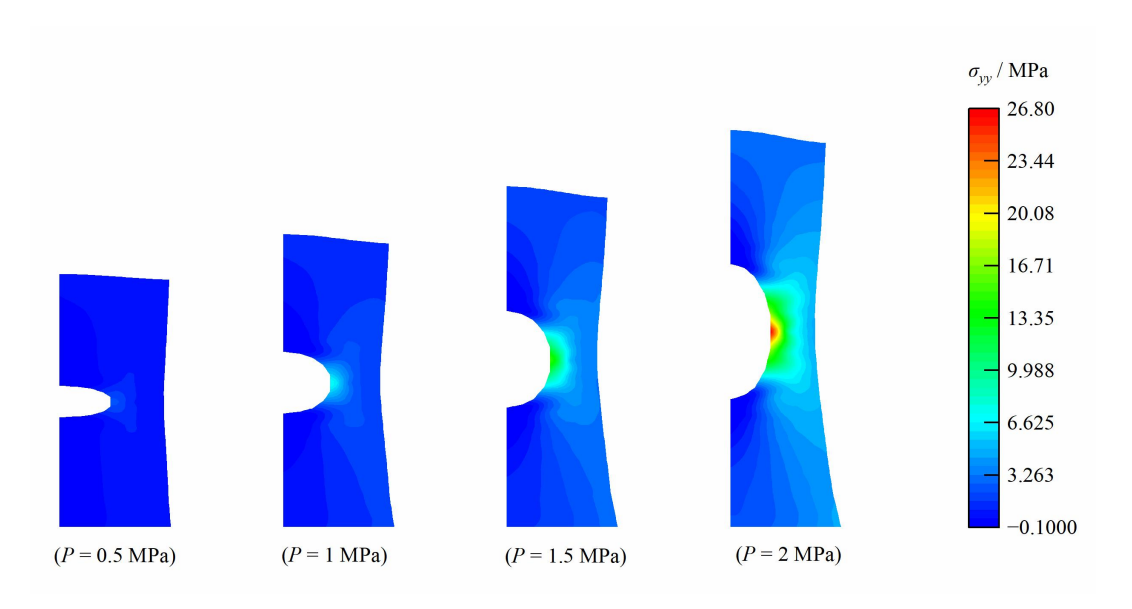


Figure 6. Stress σ_{yy} and deformation contour

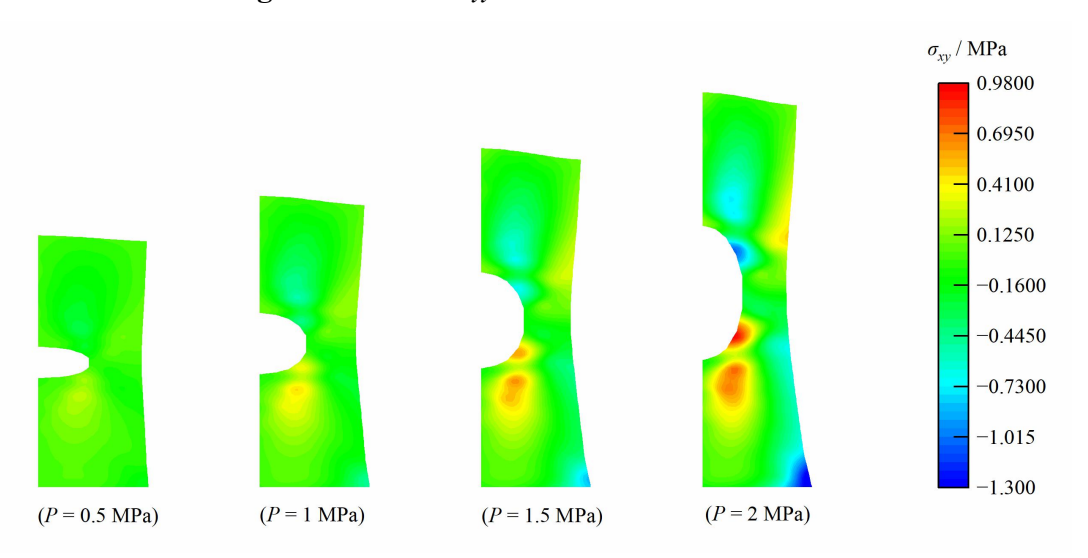


Figure 7. Stress σ_{xy} and deformation contour

Conclusions

A new BFEM based on the complementary energy principle is proposed, which can be used to solve finite strain and finite deformation problems of incompressible hyperelastic materials. The control equations for solid elements are derived by taking stationary values on complementary energy functional. The control equation contains unknown parameters, and the nonlinear mapping between variables and unknown parameters can be replaced by pretrained BP neural networks. The pre-trained BP neural network model is embedded into the BFEM calculation process to simulate the mechanical response of incompressible hyperelastic materials. The following conclusions were drawn:

- 1. In the derivation process, formulas are represented by tensors, with concise symbols and easy programming calculations. The stress tensors involved are not approximated by interpolation functions but are expressed using specific formulas composed of base force.
- 2. Due to the uncertainty of the specific form of the complementary energy function of elements, any form with J_{1T} and J_{2T} as variables can be used. Therefore, the element compliance matrix of hyperelastic materials proposed in this paper is a general expression.

- 3. The constitutive model of hyperelastic materials is replaced by a pre-trained BP neural network. When BFEM is used to simulate different hyperelastic materials, only the provided samples need to be modified and retrained.
- 4. The Mooney-Rivlin model is used to provide test samples in numerical calculations. These samples are further inverted to obtain pre-trained BP neural networks. The predicted parameters \hat{w}_{1t}^k and \hat{w}_{2t}^k are substituted into the general compliance matrix expression for calculation. This enables BFEM to accurately simulate the mechanical response characterized by the Mooney-Rivlin model, which also confirms the strong universality of the compliance matrix expression.

Acknowledgments

This work is supported by the National Natural Science Foundation of China (10972015, 11172015), Beijing Natural Science Foundation (8162008), and the Pre-exploration Project of Key Laboratory of Urban Security and Disaster Engineering, Ministry of Education, Beijing University of Technology (USDE201404).

Reference

- [1] E. Reissner, On a Variational Theorem for Finite Elastic Deformations, Studies in Applied Mathematics 32(2) (1953) 129–135.
- [2] Y.J. Peng, Y.H. Liu, Advances in the Base Force Element Method, Springer, Singapore, 2019.
- [3] Y.C. Gao, A new description of the stress state at a point with applications, Archive of Applied Mechanics 73(3-4) (2003) 171-183.
- [4] Y.J. Peng, Z.H. Li, M.M.A. Kamel, Geometrical nonlinear problems of truss beam by base force element method, International Journal for Numerical Methods in Engineering 122(18) (2021) 4793-4824.
- [5] Z.H. Li, Y.J. Peng, The base force element method based on the arc-length method for stability analysis, International Journal of Non-Linear Mechanics 144 (2022).
- [6] R.S. Rivlin, Large Elastic Deformations of Isotropic Materials. II. Some Uniqueness Theorems for Pure, Homogeneous Deformation, Philosophical Transactions of the Royal Society of London 240(822) (1948) 491-508
- [7] A.N. Gent, A new constitutive relation for rubber, Rubber Chemistry and Technology 69(1) (1996) 59-61.
- [8] R.W. Ogden, Non-linear elastic deformations, Engineering Analysis (1984).
- [9] M.M. Carroll, A Strain Energy Function for Vulcanized Rubbers, Journal of Elasticity 103(2) (2011) 173-187.
- [10] T. Beda, An approach for hyperelastic model-building and parameters estimation a review of constitutive models, European Polymer Journal 50 (2014) 97-108.
- [11] T.J. Pence, K. Gou, On compressible versions of the incompressible neo-Hookean material, Mathematics and Mechanics of Solids 20(2) (2015) 157-182.
- [12] S.J. Lee, R.T. Shield, VARIATIONAL-PRINCIPLES IN FINITE ELASTOSTATICS, Zeitschrift Fur Angewandte Mathematik Und Physik 31(4) (1980) 437-453.
- [13] B. Müller, G. Starke, A. Schwarz, J. Schröder, A FIRST-ORDER SYSTEM LEAST SQUARES METHOD FOR HYPERELASTICITY, Siam Journal on Scientific Computing 36(5) (2014) B795-B816.
- [14] T. Kirchdoerfer, M. Ortiz, Data-driven computational mechanics, Computer Methods in Applied Mechanics and Engineering 304 (2016) 81-101.
- [15] G. Capuano, J.J. Rimoli, Smart finite elements: A novel machine learning application, Computer Methods in Applied Mechanics and Engineering 345 (2019) 363-381.
- [16] L.T.K. Nguyen, M.A. Keip, A data-driven approach to nonlinear elasticity, Computers & Structures 194 (2018) 97-115.
- [17] Y.C. Gao, Z. Wang, Complementary energy principle for large elastic deformation, Science in China Series G-Physics Mechanics & Astronomy 49(3) (2006) 341-356.
- [18] Y.J. Peng, Y.H. Liu, Base force element method of complementary energy principle for large rotation problems, Acta Mechanica Sinica 25(4) (2009) 507-515.
- [19] M.J. Mooney, A Theory of Large Deformation. Journal of Applied Physics, Journal of Applied Physics 11(9) (1940) 582-592.